Journal of Geosciences and Geomatics, 2024, Vol. 12, No. 1, 12-23
Available online at http://pubs.sciepub.com/jgg/12/1/3
Published by Science and Education Publishing
DOI:10.12691/jgg-12-1-3

Mapping Land use/Land Cover Changes Caused by Mining Activities from 2018 to 2022 Using Sentinel-2 Imagery in Bétaré-Oya (East-Cameroon)

P. Azinwi Tamfuh[1,2,*], E. Ndah Musi[1], S.C. Nguemhe Fils[3], K.I. Ateh[1], A.B. Aye[1], E. Tata[1], L. E. Mamdem[4], B. Kenzong[2], G. D. Kouankap Nono[5], Dieudonné Bitom[2]

[1]Department of Mining and Mineral Engineering, National Higher Polytechnic Institute, University of Bamenda, P. O. Box 39 Bambili, Cameroon
[2]Department of Soil Science, Faculty of Agronomy and Agricultural Sciences, University of Dschang, P. O. Box 222, Dschang, Cameroon
[3]Institute of Geological and Mining Research, P.O. Box 4110, Yaoundé, Cameroon
[4]Department of Earth Sciences, Faculty of Science, University of Yaoundé I, P.O. Box 812, Yaoundé, Cameroon
[5]Department of Geology, Higher Teacher Training College, P.O. Box 20, Bamenda, Cameroon
*Corresponding author: aprimus20@yahoo.co.uk

Received February 20, 2024; Revised March 22, 2024; Accepted March 29, 2024

Abstract Artisanal mining is often associated with land use and land cover (LULC) changes like deforestation, open pits, health hazards, heavy metals contamination of land, land degradation, dust and noise pollution, soil instability, climate change, etc. This research aims to monitor LULC changes between 2018 and 2022 in East Cameroon due to artisanal gold mining activities, assessing the dynamics between LULC change types and the extent of change with time. Sentinel-2 images for 2018, 2020, and 2022 were used to examine LULC patterns at per-pixel scale with a post-classification change detection technique based on a cross matrix of changes. Supervised classification was carried using maximum likelihood algorithm of five LULC classes (bare land, vegetation, water bodies, settlements and mining activities). The results revealed spatio-temporal change patterns that have taken place in Betare-Oya. It was observed that the area under mining activities has increased from 2042.32 ha in 2018 to 3197.03 in 2020 and experienced a sharp decline to 2008.72 ha in 2022 probably as a result of the COVID-19 pandemic; with an overall percentage change from 3.95 % to 6.18 % and 3.89 % for 2018, 2020 and 2022, respectively. Also, results showed the change in vegetation from 21718.36 ha in 2018 to 16189.78 ha in 2020. In 2022, vegetation slightly increased to 16563.88 ha as a result of the fluctuation in mining activities, showing an inverse interaction between mining activities and vegetation. This study emphasizes the usefulness of Sentinel-2 data and highlights the data processing methods for long-term monitoring of the impacts of artisanal mining activities on the environment. This research will add to already existing database on LULC changes in Cameroon as a result of mining activities.

Keywords: *Sentinel-2 Imagery, LULC changes, artisanal mining, Spatio-Temporal maps, East Cameroon*

Cite This Article: P. Azinwi Tamfuh, E. Ndah Musi, S.C. Nguemhe Fils, K.I. Ateh, A.B. Aye, E. Tata, L. E. Mamdem, B. Kenzong, G. D. Kouankap Nono, and Dieudonné Bitom, "Mapping Land use/Land cover Changes Caused by Mining Activities from 2018 to 2022 Using Sentinel-2 Imagery in Bétaré-Oya (East-Cameroon)." *Journal of Geosciences and Geomatics*, vol. 12, no. 1 (2024): 12-23. doi: 10.12691/jgg-12-1-3.

1. Introduction

Exploration and exploitation of mineral resources is one of the common activities through which the environment suffers damages; through excavation for trenching, and reworking of sediments for the search of alluvial minerals through artisanal activities [1]. Mining activities are reported to have detrimental effects on land [2]. Overburden removal of leads to significant deforestation and arable land as more land is exposed to erosion [3]. Water bodies are also affected [4]. This land degradation causes alteration in ecological and economic functions [1]. Land degradation is one of the most common consequences of mining activites most often leading deforestation, open pits, health hazards, heavy metals contamination of land and water, dust and noise pollution and soil instability [5]. Other consequences of artisanal gold mining operations are floods, sedimentation and landscape modifications [6]. Miners often abandon the previous mining area without any land restoration. Increase in land conversion due to mining operations is a threat to agricultural sustainability [3,7]. Information on real extent of land degradation due to mining operations is vital for policy conservation [8]. However, this type of

data is rarely available for large areas [9]. It is thus essential to map the extent and severity of soil degradation due to gold mining activities [5]. One of the best approach to land mapping is spatial remote sensing as it is faster, cost-effective, can easily cover large surface areas and the uncertainty level of the maps generated can be determined with high precision. Various versions of GIS and remote sensing approaches exist like geostatistics, multi-criteria GIS, Analytical Hierarchy Process (AHP), Analytical Network Process (ANP), Simple Additive Method (SAM), Weighted Linear Combination (WLC), Multi-Criteria Decision Analysis (MCDA) and Unclear Logic [9]. Remote sensing has been reported as the most effective, fastest and least expensive way to evaluate land degradation [10]. Sentinel-2 is ESA's medium spatial resolution super-spectral instrument aimed at ensuring data continuity for global land surface monitoring of Landsat and SPOT and it enables to monitor vegetation after mine closure [10]. Normalized difference vegetation index (NDVI) is the most suitable index to monitor changes in vegetation cover as it is least affected by topographic factors and is indicative of the plant photosynthetic activity [11]. Reliable temporal data on the impact of mining activities are required to aid in mine reclamation and management efforts [12]. Land degradation as a result of artisanal mining in the eastern part of Cameroon has reported [5,11,12,13,14]. Since land degradation is a continuous process as well as mining activities, it is therefore necessary to continually study the changes over time in gold-based mining district such as the eastern region as well as make endeavours to narrow this research to small size artisanal mining communities such as Bétaré Oya. The world depends on agriculture for food and sustenance. Agricultural success entails the availability of fertile soils or land [7]. Land degradation reduces the fertility of land and such aspects include erosion, deforestation, mining and settlement. Mining activities are also increasing the impact of land degradation. In areas where mining activities are prominent such as in Betare-Oya, there is an influx of people leading to increasing settlement in the area. In as much as land degradation can be evaluated manually, regular monitoring and preparing LULC maps by conventional methods is time consuming, expensive, labour intensive and carrying out ground surveys may also be difficult in some areas due to terrain characteristics [1]. Thus, a more rapid but accurate method for this evaluation is needed. Rapidness comes in as a result of the changing times and with an advance in technological development, it is necessary that every aspect of mining be incorporated in technology for rapid results which are accurate and can maximize time. This work aims to evaluate the extent of land degradation in Betare-Oya as a result of mining activities between 2018 and 2022 using Geographic Information System (GIS) and remote sensing technologies precisely Sentinel-2 Imagery. The key objectives of this waork are (1) to produce maps of spatial distribution and expansion of land use patterns; (2) identify changes in land with time due to mining activities; and (3) finally to establish the link between mining activities and land degradation in the studied area. The results obtained will enable stakeholders to predict the extent and rate of land degradation over time as a result of mining activities with possible methods of rehabilitation and restoration of land due to land degradation proposed as per the results obtained, to counteract the effects of mining activities in this area.

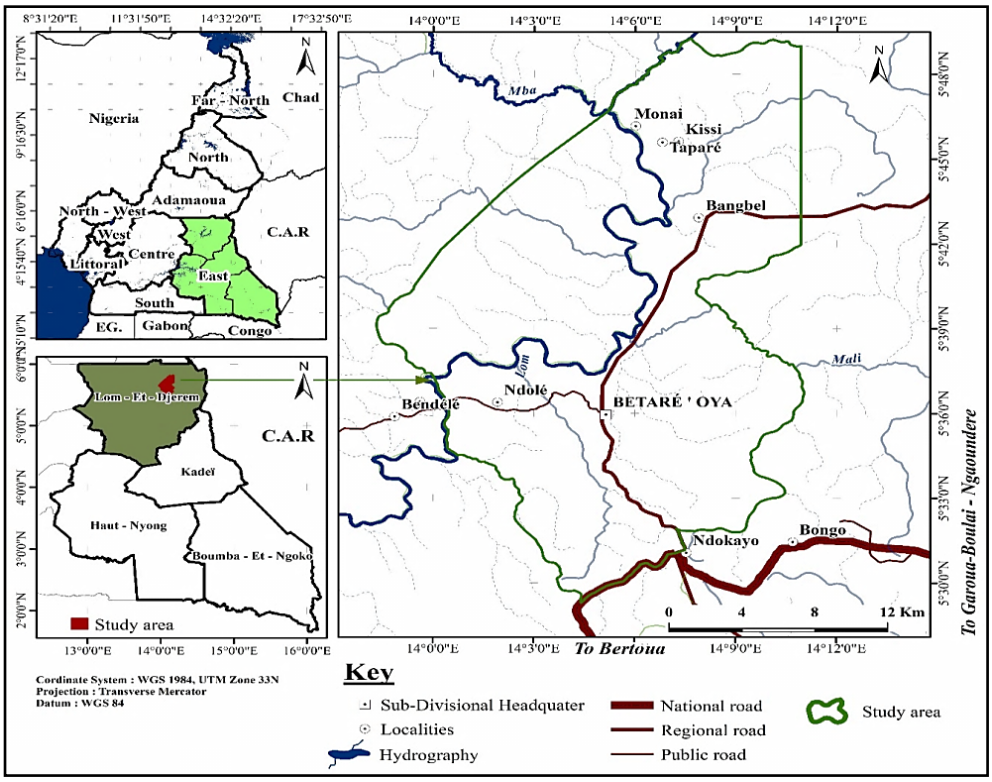

Figure 1. Location map of Betare-Oya in East Cameroon

2. Materials and Methods

2.1. Study Site

Betare-Oya is located in the East Region of Cameroon in the Lom and Djerem Division, between latitude 14°1'0.643"E and longitude 5°42'48.587"N (Figure 1). Betare-Oya is located 180 km from Bertoua with a surface area of 12,000 km^2 [16]. The wet season is warm, oppressive, and overcast and the dry season is hot and mostly cloudy [16,17]. It is characterized by an average annual temperature of 31.59^{o}C and an average annual precipitation of 2198.78 mm. It has four seasons: a long rainy season (mid-August to mid-November), a long dry season (mid-November to February), a short rainy season (March to May) and a short dry season (July and mid-August). The vegetation in Betare-Oya portrays the presence of an ecotone, marking the transition between the humid equatorial forest of the Centre, South and East regions of Cameroon with the shrubby savannah of Adamawa. The vegetation cover alternates between islands of forest galleries, particularly along the water courses and a savannah peri-forest dotted with relatively dense shrubs and in places of anthropogenic origin [17]. The hydrography Betare-Oya consists of very dense drainage pattern belonging to the Sanaga watershed. The main river is the Lom which is woven around an interesting network of rivers, some of which are the Mba and Mali Rivers, which pour into the Lom. The morphological conditions of this environment influence the hydrography. Almost all rivers flow in a north-south direction. It is along the line of these rivers that semi-mechanized and artisanal gold mining is concentrated. The relief is relatively rugged characterised by dotted hills here and there. It is characterized by an altitudinal range between 658 m and 1072 m and an average altitude of about 834 m. The low lands fall within the Lom basin and the highlands surrounding these lowlands. Ferrallitic soils with red facies, ocher to yellow, thin and stony form the major soil type in the area. Hydromorphic soils are located in the lowlands. Betare-Oya area is part of the Neoproterozoic (700 - 1100 Ma) volcano-sedimentary formations of Cameroon or schist belts referred to as the lower Lom series. These formations occur discordantly on the Pan-African basement made up of migmatites and granitic to ortho-gneissic and biotite rich rocks; they are confined to the NE-SW trending shear zones as part of the Central African and Cameroon shear zone system along which granitic plutons are common [18,19,20]. The municipality has an estimated population of around 41,173 inhabitants spread over 59 villages. These villages are grouped into 3 sections: Laï, Yayoué and Bitom. The economic environment is organized around extractive activities (gold, sand and precious stones), agriculture and a little hunting. Indeed, Betare-Oya is the epicentre of mining in the East Region. This mining is also accompanied by logging. Far from the mining sites, subsistence family farming, fishing, crafts and small trade are deployed, the actors of which are closely dependent on mining activities. Finally, artisanal hunting is also highly developed [17].

2.2. Methods

2.2.1. Presentation of Sentinel-2

The main features of Sentinel-2 are compiled in Table 1. Sentinel-2 is a European wide-swath, high-resolution, multi-spectral (MS) imaging mission. The full mission specification of the twin satellites flying in the same orbit but phased at 180° is designed to give a high revisit frequency of 5 days at the Equator. It carries an optical instrument payload that samples 13 spectral bands: four bands at 10 m, six bands at 20 m and three bands at 60 m spatial resolution. The orbital swath width is 290 km. The twin satellites of SENTINEL-2 provide continuity of SPOT and LANDSAT-type image data, contribute to on-going multispectral observations and benefit Copernicus services and applications such as land management, agriculture and forestry, disaster control, humanitarian relief operations, risk mapping and security concerns [21,22]. The Sentinel-2 mission offers an unprecedented combination of systematic global coverage of land surfaces, a high revisit of five days at the equator under the same viewing conditions, high spatial resolution (10, 20 and 60 m depending on bands) and a wide field of view for multispectral observation from 13 bands in the Visible, Near infra-red and Shortwave infra-red part of the electromagnetic spectrum. The 13 spectral bands span from Visible and Near infra-red to Shortwave infra-red featuring: (1) four bands at 10 m: the classical blue (490 m), green (560 m), red (655 m), near-infrared (842 m) bands dedicated to land applications; (2) six bands at 20 m: 4 narrow bands in the vegetation red edge spectral domain (705 nm, 740 nm, 775 nm and 865 nm) and 2 SWIR bands (1610 nm and 21 nm) 90 dedicated to snow/ice/cloud detection and to vegetation moisture stress assessment; and (3) three bands at 60 m dedicated to atmospheric correction (443 nm for aerosols and 940 for water vapour) and to cirrus detection (1380 nm). The obit is sun synchronous at 78 km altitude (14 + 3/10 revolutions per day) with a 10:30 a.m. descending mode. This local time was selected as the best compromise between minimizing cloud cover and ensuring suitable sun illumination [23].

Table 1. Sentinel 4 Bands, wavelength and resolution [21]

Sentinel-2 bands	Characteristic	Sentinel-2A		Sentinel-2B		Spatial resolution (m)
		Central wavelength (nm)	Bandwidth (nm)	Central wavelength (nm)	Bandwidth (nm)	
1	Coastal aerosol	442.7	21	442.2	21	60
2	Blue	492.4	66	492.1	66	10
3	Green	559.8	36	559.0	36	10
4	Red	664.6	31	664.9	31	10
5	Vegetation red edge	704.1	15	703.8	16	20

Sentinel-2 bands	Characteristic	Sentinel-2A		Sentinel-2B		Spatial resolution (m)
		Central wavelength (nm)	Bandwidth (nm)	Central wavelength (nm)	Bandwidth (nm)	
6	Vegetation red edge	740.5	15	739.1	15	20
7	Vegetation red edge	782.8	20	779.7	20	20
8	NIR	832.8	106	832.9	106	10
8A	Narrow NIR	864.7	21	864.0	22	20
9	Water vapour	945.1	20	943.2	21	60
10	SWIR – Cirrus	1373.5	31	1376.9	30	60
11	SWIR	1613.7	91	1610.4	94	20
12	SWIR	2202.4	175	2185.7	185	20

Table 2. Characteristics of downloaded images

Nº	Satellite	Level of product	Band used	Resolution (m)	Date of image	Time	Phenological cycle
1	Sentinel-2B	L1C	2,3,4,8,11,12	20	10/03/2018	11:27:45	Dry Season
2	Sentinel-2B	L1C	2,3,4,8,11,12	20	28/02/2020	09:35:09	Dry Season
3	Sentinel-2B	L1C	2,3,4,8,11,12	20	27/02/2022	09:35:33	Dry Season

2.2.2. Mapping Process of LULC Patterns

Image Download: Three Sentinel-2B images were downloaded from Earth explorer websites within the same period of the year for 3 different years; 2018, 2020 and 2022 (Table 2). The chosen period was February (2020/2022) and March 2018. This choice was guided by the search for same good quality images with same phenological cycle, dry season and good images with no cloud cover. Sentinel-2 images with similar spatial resolution of 20 m enabled mapping of major LULC pattern (vegetation, bare land, water bodies, settlement and mine activity areas

- *Data pre-processing:* Satellite image transformations involve manipulations of multiple band data in order to highlight particular properties or features of interest within the study area, in a better and more effective way than the original input images.
- *Layer stacking:* Layer Stacking was done for each of the 3 sentinel-2 images using Envi 5.7. Layer stacking involves combining multiple image layers (only layers with similar number of rows and number of columns) into a single image. Bands with different spatial resolution were resampled so as to the target resolution. All sentinel bands with spatial resolution of 10 m (that is band 2, 3, 8 and 12) were resampled to 20 m.
- *Geometric correction:* It is necessary to correct geometric distortions caused by sensor-Earth geometry variations and conversion of the data to real geographic coordinates (longitudes and latitudes). When a number of images are to be used together, they are georeferenced.

Image-to-image registration method was conducted to match the images so that they could be as comparable as possible in terms of geometric and radiometric qualities. All data were projected to the Universal Transverse Mercator projection system (zone 32N) and to World Geodetic System 84 datum in order to ensure consistency between datasets.

- *Image Enhancement:* Image enhancement enables improve the appearance of the image to assist in visual interpretation and analysis. Enhancement functions included contrast, stretching to increase the tonal distinction between features, and spatial filtering to enhance or suppress specific spatial patterns in the image. Also, different colour composites (4-3-2, 8-4-3 and 4-8-3, 5-4-3 bands, for RGB channels) enabled to enhance the identification of features so as to select training set or classification signatures to be used.
- *Selection of training set as defined by* [24,25]: Sample polygons were created for each image (2018, 2020 and 2022) based on visual interpretation on the image to recognize the LULC feature classes. Every spectral analogous sub-area was demarcated with specified class name using a training set.
- *Image Classification:* According to [26], **image classification** operations are used to digitally identify and classify pixels in the dataset. **It** is usually performed on multi-channel datasets (A) and this process assigns each pixel in an image to a particular class or theme (B) based on statistical characteristics of the pixel brightness values. After selecting the training sample/sets, they were satisfactorily reviewed. Supervised classification was done using the maximum likelihood classification classifier (MLC) which is the most common efficient statistical technique for evaluating the standard LULC classifications. By the classification, five LULC types were recognized (vegetation, bare land, water bodies, mining activities and settlement).
- *Accuracy Assessment:* The steps as proposed by [26,27] were used to assess the accuracy of the classification involving 150 random points. Thus, pixels to be sampled were randomly selected and selected points are transferred from the satellite image to Google earth pro thereby creating a kml file. Alternatively, Google Earth map can be used in ArcGIS as a base map. Sample points were interpreted on the Google earth, the interpretation is compared to the classification results and correctly classified pixels are tabulated. The overall accuracy of the classified image compares how each of the pixels is classified versus the definite land cover

conditions obtained from their corresponding ground truth data.

Producer's accuracy measures errors of omission, which is a measure of how well real-world land cover types can be classified.

$$\text{Product's Accuracy} = \frac{\text{Number of Correctly Classified Pixels in each Category}}{\text{Total Number of Reference Pixels in that Category}} x100 \quad (1)$$

User's accuracy measures errors of commission, which represents the likelihood of a classified pixel matching the land cover type of its corresponding real-world location.

$$\text{User's Accuracy} = \frac{\text{Number of Correctly Classified Pixels in each Category}}{\text{Number of Correctly classified Pixels in that Category}} x100 \quad (2)$$

$$\text{Kappa Coefficient}(T) = \frac{\left((TS \times TCS) - \sum(\text{Column Total} * \text{Row Total})\right)}{\left(TS^2 - \sum(\text{Column Total x Row Total})\right)} x100 \quad (3)$$

The interpretation of the Kappa coefficient is done according to [28] as compiled in Table 3.

Table 3. Interpretation of agreement for kappa coefficient [28]

Value of kappa-hat	Interpretation of agreement
$0.8 \leq k \geq 1$	Almost perfect agreement
$0.61 \leq k \geq 0.8$	Substantial agreement
$0.41 \leq k \geq 0.60$	Moderate agreement
$0.21 \leq k \geq 0.0.40$	Fair agreement
$0.0 \leq k \geq 0.20$	Slight agreement
$k < 0.0$	Poor agreement

2.2.3. Detection of change in LULC

A post-classification enabled to quantify the overall land cover changes between 2018 and 2022 into categories as shown in Table 4.

Table 4. LULC classes and their description

N°	LULC Classes	Description
1	Bare Land	Bare land refers to areas with no dominant vegetation cover on at least 90 % of the area. That is land surfaces with exposed soil as caused by human activities and/or natural causes. Areas exposed by activities such as farming and mining activities where the tops soil has been excavated leaving it void of vegetation are also considered here.
2	Vegetation	Vegetation is an assemblage of plant species and the ground cover they provide. It comprises of the nine Vegetation Formation Group types which are divided as Forest, Shrubland, Herbaceous vegetation, Desert, Swamp & Aquatic Vegetation, Alpine Tundra and Sparse Vegetation, Cultivated Vegetation, Urban Vegetation, and Non-Vegetated Area.
3	Water Bodies	Water Bodies means any natural or artificial inland body of water or expanded part of a water course, including lakes, ponds and reservoirs. It also encompasses standing ponds or dams made by man intentionally or unintentionally through activities such as artisanal mining
4	Mining activities	These are areas where artisanal mining of gold is being carried out either by individuals or artisanal companies.
5	Settlement	This is the place, typically one which is being inhabited by the human community, where people have established.

In summary, the processing procedure begins with identifying real-world data as follows: extract images, identify the location of the study area, identify the composite band for satellite processing, identify construct layers form, and finally identify the classifiers. The statistical results and overall classification accuracy are calculated for each image for each satellite as shown in Figure 2.

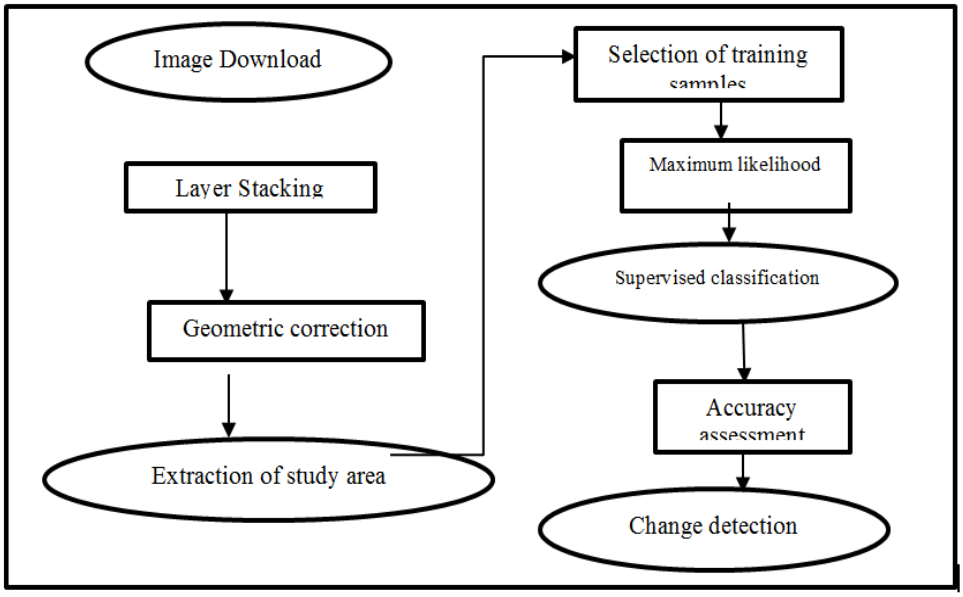

Figure 2. Flowchart of the method used

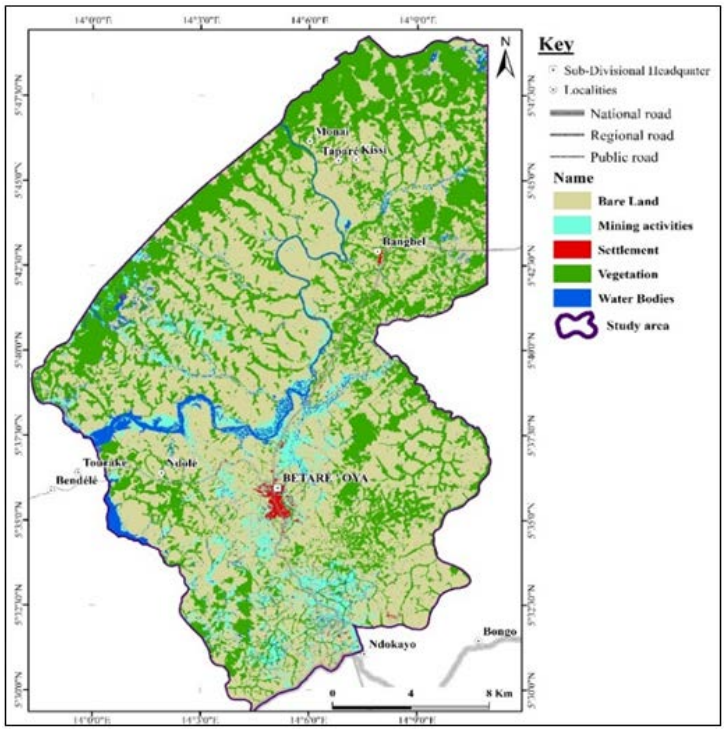

Figure 3. LULC map 2018 of Betare-Oya

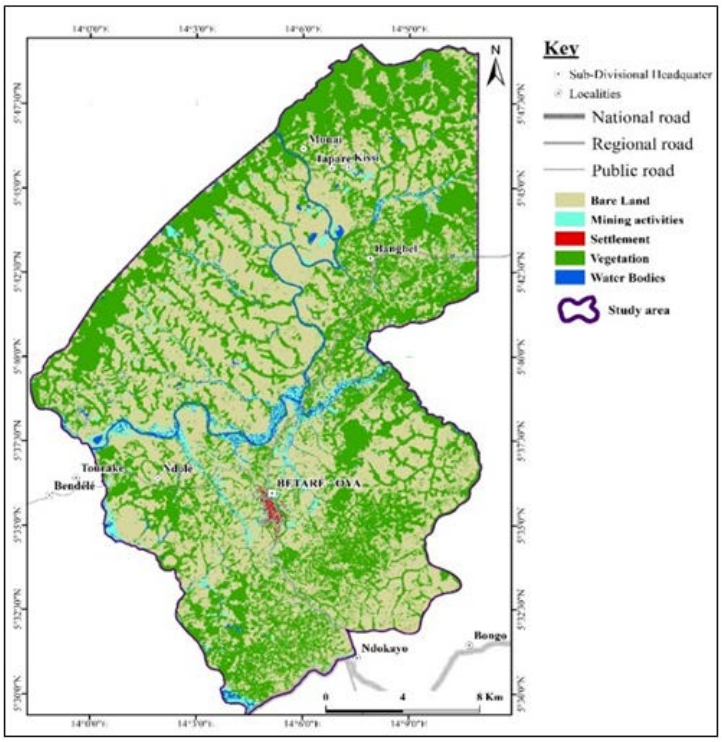

Figure 4. LULC map for 2020

3. Results and DISCussions

3.1. Results

3.1.1. Spatial Distribution and Expansion Maps of Land Use/Land Cover Patterns

The spatial distribution and expansion analysis of the LULC for 2018 were gotten and presented as spatial map (Figure 3). An overall area of 51692.59 ha constituted the total of classification (Table 5). In 2018, Bare land, Mining activities, Settlement, Vegetation and Water Bodies occupied an area of 26481.66 ha (51.23 %), 2042.32 ha (3.95 %), 105.57 ha (0.20 %), 21718.36 ha (42.01 %) and 1344.68 ha (2.60 %), respectively, with bare land occupying the majority of the area and settlement being the least. The spatial distribution and expansion analysis of the LULC for 2020 were gotten as presented below in the spatial map (Figure 3) and accompanying statistics (Table 5).

Table 5. LULC classes

N°	Class	Area (ha)	Percentage (%)
2018			
1	Bare Land	26481.66	51.23
2	Mining activities	2042.32	3.95
3	Settlement	105.57	0.20
4	Vegetation	21718.37	42.01
5	Water Bodies	1344.69	2.60
2020			
1	Bare Land	29936.48	57.91
2	Mining activities	3197.02	6.18
3	Settlement	287.63	0.56
4	Vegetation	16189.78	31.32
5	Water Bodies	2081.68	4.03
2022			

In 2020, Bare land, Mining activities, Settlement, Vegetation and Water Bodies occupied an area of 29936.48 ha 3197.02 ha, 287.63 ha, 16189.78 ha and 2081.68 ha, respectively, with overall percentages of 51.97 %, 6.18 %, 0.56 %, 31.01 % and 4.03 %, respectively, with bare land still occupying the largest portion and settlement occupying the least portion. As compared to 2018, it is observed that there is an increment in the percentage of most classes (mining activities from 3.95 to 6.18 %, bare land from 51.23 to 57.91 %, Water bodies and 2020, followed by vegetation with an area of 16563.88 ha and percentage of 32.04 %, meanwhile water bodies, mining activities and settlement occupy an area of 1627.52 ha (3.15 %), 2008.72 ha (3.89 %) and 325.440 ha (0.63 %). Settlement remains the least represented of all LULC classes with 0.63 %.

3.1.2. Change Detection to LULC Aspects in Betare-Oya

The results the evolution of the different LULC classes in 2018, 2020 and 2022 (Figure 5, Figure 6 and Figure 7) enable to view actual areas of change. Across the statistics (Table 6), it is noticed that, progressively from one year to another, change takes place in that, a particular area occupied by a particular LULC class experiences change as proportions of it changes to any of the other LULC classes and as proportions of these other classes are being changed to that LULC class as well.

In Table 6 and Figure 5, it is observed that from 2018 to 2020, Bare land increased 26481.66 to 29936.48 ha, mining activities increased from 2042.32 to 3197.02 ha, settlement had a sharp increase from 105.56 to 287.63 ha, vegetation also decreased from 21718.36 to 16189.78 ha and water bodies increased from 1344.68 to 2081.68 ha.

A difference classes from 2020 to 2022 (Table 6) reveals that bare land increased from 29936.48 to 31167.04 ha, meanwhile mining activities decrease from 3197.03 to 2008.72 ha with a great part of changed area (2139.44 ha) being changed into bare land in 2022; settlement increases from 287.63 to 325.44 ha, vegetation also increases from 16189.78 to 16563.88 ha and water bodies decline from 2081.68 to 1627.52 ha with a major part of the changed area being converted to bare land in 2022.

From the above statistics, overall change showing evolution from 2018 to 2022 is demonstrated as from 2018 where bare land occupied an area of 26481.66 ha and in 2022, it changed to 31167.04 ha (Figure 8; Table 6). This sequence of change continues as mining activities decrease from 2042.32 ha in 2018 to 2008.72 ha in 2022, settlement sharply rising from 105.57 in 2018 to 325.44 ha in 2022, a reduction is demonstrated as vegetation reduces from 21718.36 in 2018 to 16563.88 and water bodies rising from 1344.69 in 2018 to 1627.52 ha in 2022.

3.1.3. Accuracy Assessment

The results obtained from the classification accuracy assessment computed to get the Kappa value for the classification are presented in Table 7 for the three classifications for 2018, 2020 and 2022.

Table 6. LULC change statistics from 2018-2020, 2020-2022 and 2018 to 2022

Classes	Year	Bare Land	Mining activities	Settlement	Vegetation	Water Bodies	Grand Total
Year		2020					
Bare Land	2018	22925.96	1988.26	76.47	925.551	563.25	26481.66
Mining activities		894.94	580.79	111.22	84.19	364.69	2042.32
Settlement		7.28	12.66	83.831	0.38	1.41	105.57
Vegetation		5741.68	522.907	18.26	14915.08	515.68	21718.36
Water Bodies		362.43	91.074	3.11	228.27	654.13	1344.68
Grand Total		29936.48	3197.02	287.63	16189.78	2081.68	51692.59
year	2020	2022					
Bare Land		26493.48	804.70	73.21	2251.68	304.359	29936.48
Mining activities		2139.44	731.88	77.00	117.872	128.470	3197.03
Settlement		71.130	53.587	162.48	3.836	1.984	287.63
Vegetation		2105.86	33.16	5.79	13689.19	310.266	16189.78
Water Bodies		692.88	208.59	6.53	311.59	877.049	2081.68
Grand Total		31167.04	2008.72	325.44	16563.88	1627.52	51692.59
year	2018	2022					
Bare Land		24259.30	1016.20	91.50	892.73	210.98	26481.66
Mining activities		994.11	548.69	125.46	83.85	281.13	2042.32
Settlement		7.96	16.93	79.26	0.14	1.26	105.57
Vegetation		5871.72	152.99	24.89	15184.86	463.02	21718.36
Water Bodies		364.18	96.32	3.51	208.01	663.06	1344.69
Grand Total		31167.04	2008.72	325.44	16563.88	1627.52	51692.59

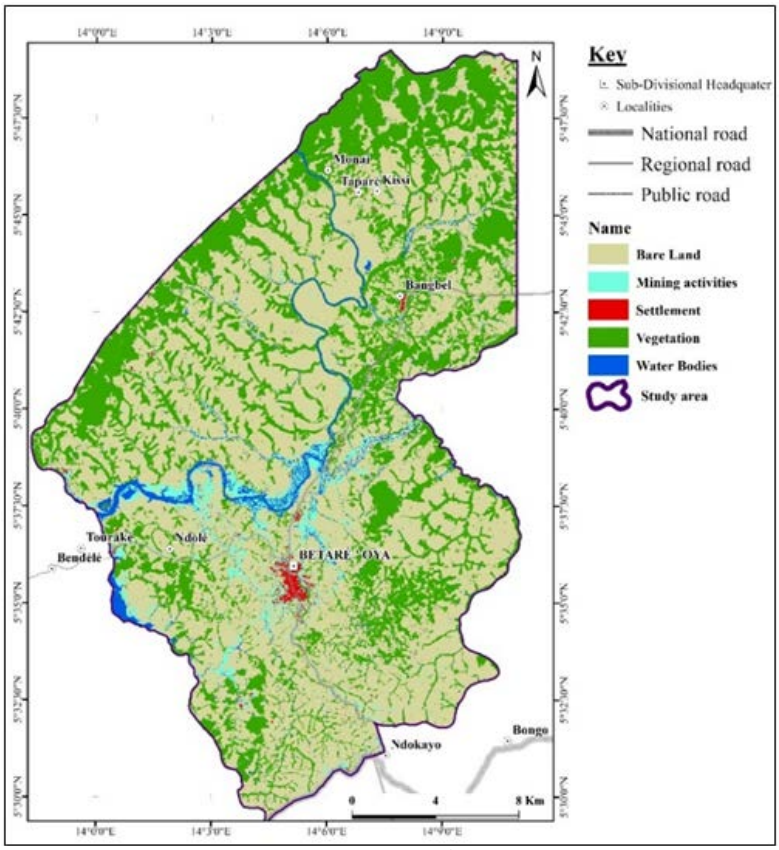

Figure 5. LULC map for 2022

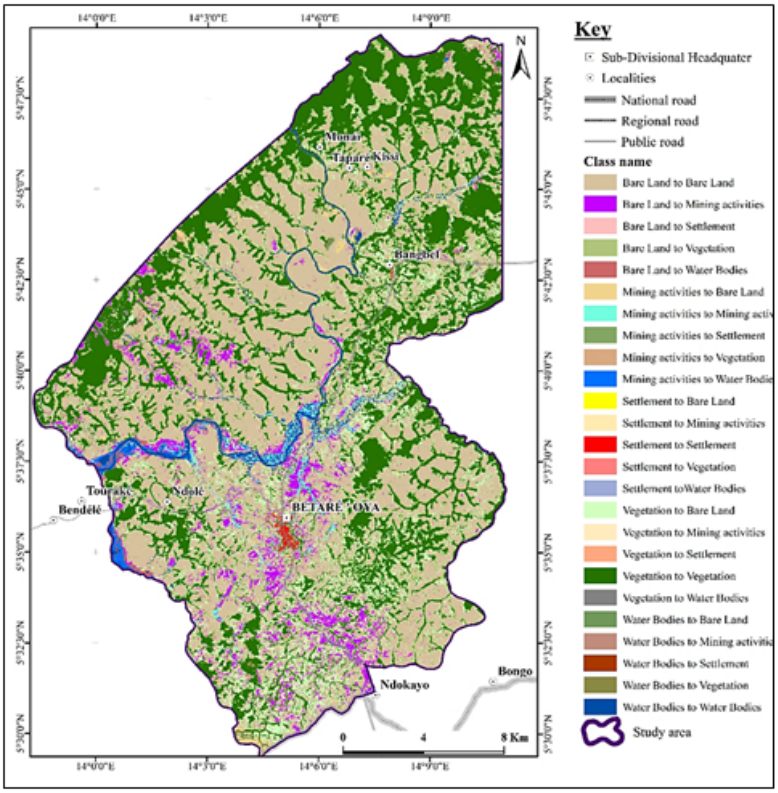

Figure 6. LULC change from 2018-2020

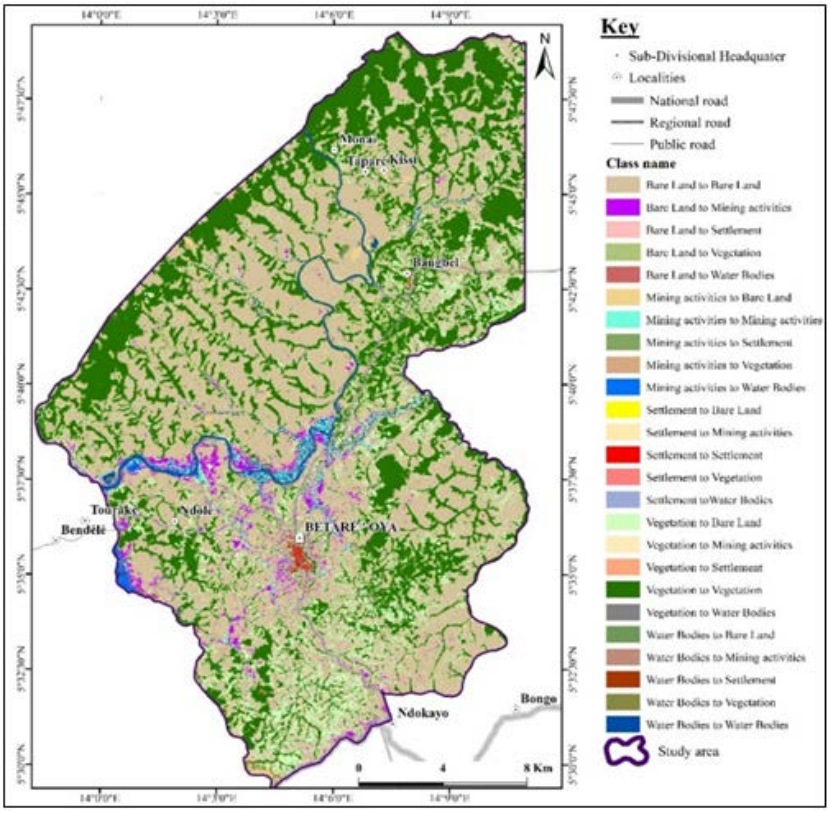

Figure 7. LULC change from 2020-2022

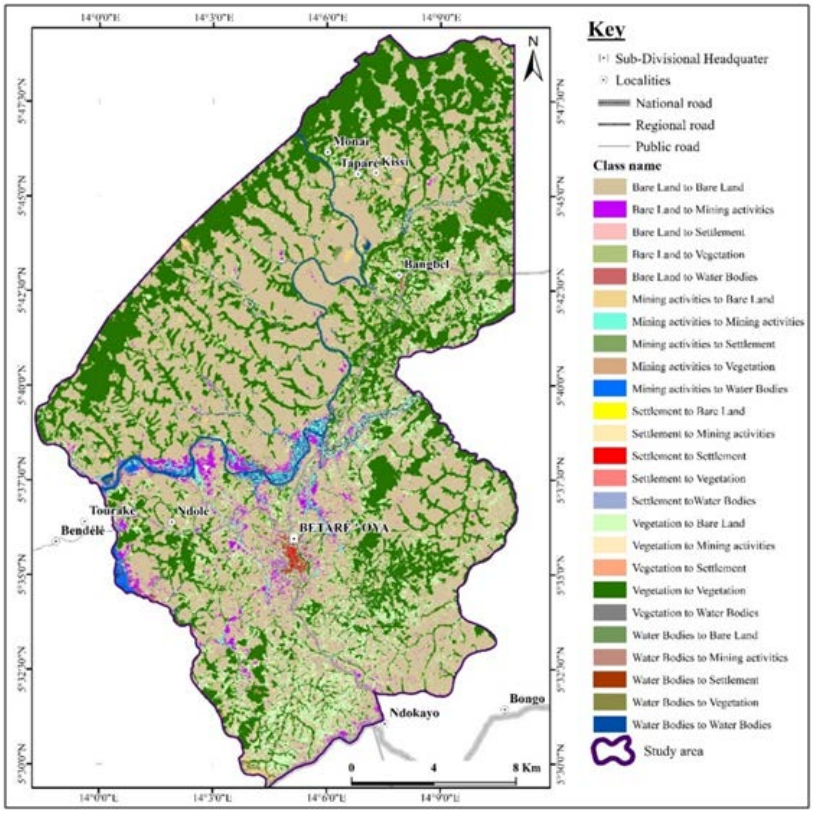

Figure 8. LULC change from 2018-2022

Table 7. Accuracy assessment statistics

Class Name	User's Accuracy (%)	Producer's accuracy (%)
2018		
Bare Land	72.41	80.77
Vegetation	86.36	67.86
Water Bodies	40	100
Settlements	83.33	100
Mining activities	50	33.33
Overall accuracy	75%	
K_c	0.61	
2020		
	`	
Bare Land	76.9	85.7
Vegetation	86.9	77.9
Water Bodies	81.3	76.5
Settlement	100	100
Mining Activities	50	
Overall accuracy	80.23%	
K_c	0.69	
2022		
Bare Land	70.24	100.00
Vegetation	100	70.59
Water Bodies	85.71	85.71
Settlement	75	100.00
Mining Activities	80	80.00
overall accuracy	82.63%	
K_c	0.79	

3.2. Discussion

3.2.1. Analysis of spatial distribution and expansion of LULC in Betare- Oya

Artisanal gold mining activities are known to have adverse and degrading effects on the land, its landscapes as well as environment (Tehna et al., 2015). This research has evaluated the changes on land due to artisanal gold mining activities in Betare-Oya using Sentinel-2 imagery. Sentinel-2 imagery as a continuation of the Landsat and spot (ESA, 2022) has been used to evaluate land cover changes (Farah et al., 2021). Spatial distribution maps were drawn from the classification of three Sentinel-2 images where they displayed the clear distribution of land cover classes over the years. It is observed that vegetation in Betare-Oya is more prominent along river courses and valleys. Likewise, mining activities appear to be prominent along the Lom and other river courses suggesting that vegetation, water bodies and mining activities has an interactive relationship. Previously, the relationship between mining activities and vegetation had been shown where the growth in mining activities was at the expense of vegetation [5].

It is also observed that mining continues to be dominant in the northern part of Betare-Oya [5], but has also emerged and spread to the west and south of Betare-Oya. Bare land is observed to be continually increasing across the years in Betare-Oya with a dominant percentage of 51.23 %, 57.91 % and 60.29 %, for 2018, 2020 and 2022 respectively, showing a trend of continuous increase in bare land over time. This observation is in agreement with the findings of [5]. This bare land can be affiliated to the season of choice when this research was being done. In the dry season when this work was done, there is less vegetation. Moreover, continuous increase in bare land can be attributed to the fact that more vegetation (forest) is being wiped out for mining activities and water bodies exhausted by such practices. During artisanal gold mining, miners cut the plants to get enough space to carry out their activity causing deforestation and more land is exposed. The increasing population with a percentage trend of 0.20 %, 0.57 % and 0.63 % for 2018, 2020, and 2022, respectively will lead to increase agricultural land use (bush burning and fallowing) and increase bare land [29].

An assessment of the changes on the five LULC classes from 2018 to 2020 shows an increase in bare land from 26481.66 to 29936.48 ha which could be linked to the increase in mining activities from 2042.32 to 3197.02 ha as well as increase in settlement from 105.56 to 287.63 ha and a reduction in vegetation from 21718.36 to 16563.88 ha. Mining activities result in an increase in settlement and enhances forest destruction, hence reduction in vegetation [5,15]. There is also an increase in water bodies from 1344.68 to 2081.68ha and this can also be related to increase mining activities as more ponds are created during artisanal gold mining for panning.

Further analyses of the changes in Betare-Oya with time from 2020 to 2022 showed an increase in bare land from 29936.48 to 31167.04 ha, an increase in settlement from 287.63 to 325.44 ha as well as vegetation increase from 16189.78 to 16563.88 ha. This increase in vegetation can be correlated to a drop in mining activities. A decline in the mining activities also led to a reduction in water bodies from 2081.68 to 1627.52 ha.

In as much as areas of mining activities keep changing to other classes with time, it continues to convert a greater portion of other classes to mining activities. The trend of change is characterized by bare land continuing to be the dominant class occupying most of the area with an increase from 26481.66 ha in 2018 to 31167.04 ha in 2022. Though mining activities experienced a drop in 2022, this did not alter the steady increase in bare land. This implies that despite the drop in its activities, the population increase (from 105.57 ha in 2018 to 325.44 ha in 2022) in Betare-Oya continues to carry out other activities such as farming which leads to increase in bare land and huge decrease in the vegetation (from 21718.36 ha in 2018 to 16563.88 ha in 2022). The increase in area occupied by water from 1344.69 to 1627.52 ha within this time frame can be affiliated to both mining and the continuous increase of water from the Lom-Pangar dam. The decrease in the area occupied by mining activities from 2042.32 ha in 2018 to 2008.72 ha in 2022 can be linked to the COVID-19 outbreak which became prevalent in Cameroon in 2020. Its effect on various sectors in the sub-Saharan African countries [29] such as the drop in the prices of minerals and others could have affected the artisanal gold mining sector in Cameroon. A challenge in this study arises from the confusion in differentiating settlement from mining activities due to their similarity in spectral reflectance.

In general, mining activities have a cordial relationship with other LCLU classes in Betare-Oya. This is affirmed by [15] that mining activities attract population increase, hence increase in settlement. It also leads to deforestation,

thus influencing both bare land and vegetation, digging of pits and creation of ponds, divert water courses and block others river channels creating diverse effects on water bodies. Thus, mining activities have a degrading effect on the land in which it steadily occupies and this can be successfully assessed and affirmed using Sentinel-2 satellite imagery.

3.2.2. Accuracy Assessment

The results of Kappa for 2018, 2020 and 2022 are in the order 0.61, 0.69 and 0.79 and the classification can be considered good according to [28,30]. Thus, the classification can be said to be in substantial agreement to ground truth. These results assert the fact that in the evaluation of land degradation in Betare-Oya, using spatial maps of the expansion and distribution of land cover classes can be successfully derived using sentinel-2 imagery treated by supervised classification [30,31,32].

4. Conclusions

This objective of this work was to map changes in land use patterns from from 2018 to 2012 caused by mining activities in Betare-Oya using Sentinel-2 images. Supervised classification by the maximum likelihood classifier method to derive the land use/land cover classes enabled to obtain five LULC classes. Th main results reveal an expansion of mining activities across the vicinity of Betare-Oya gold district, growth of mining activity over the territory in 2018 covering an area of 2042.32 ha and it quickly spread over the terrain in 2020 taking an overall area of 3197.03 ha followed by a sharp decline in 2022 with a total area of 2008.72 ha. The influence of mining activities continues to take a turn on natural vegetation and enhancing the increase in bare land. The natural vegetation shows strong relationg with the alternation in mining activities with a continuous decrease from 2018 to 2020 and an increase in 2022 due to a decline in mining activities. Mining activities and settlement have an impact on bare land as reflected by its continuous and sharp increase from 2018 to 2022, occupying the most of the terrain through the year. These findings highlights the strength of Sentinel-2 for long-term monitoring of land degradation caused by artisanal mining activities and provides results that are useful in the domain of environmental impact assessment of gold mining activities.

Conflict of Interests

The authors did not declare any conflict of interests.

References

[1] Ahmad N, Pandey P, (2018) Assessment and Monitoring Of Land Degradation Using Geospatial Technology In Bathinda District, Punjab, India Centre for Environmental Sciences and Technology, Central University of Punjab, Bathinda, Punjab-151001, India. *Solid Earth* 9: 75–90.

[2] Mbaya RP, (2013) Land Degradation Due To Mining: The Gunda Scenario International *Journal of Geography and Geology* 2(12): 144-158.

[3] Sahu HB, Er SD, (2011) Land Degradation due to Mining in India and its Mitigation Measures. In: *2nd International Conference on Environmental Science and Technology*, Feb 26-28, 2011, IEEE, and Singapore, pp. 2-20.

[4] Marangoz AM, Sekertekin A, Akçin H (2017) Analysis of land use land cover classification results derived from sentinel-2 image, in: Proceedings of the 17th International Multidisciplinary Scientific GeoConference Surveying Geology and Mining Ecology Management, SGEM, pp. 25-32.

[5] Kamga MA, Nguemhe Fils SC, Ayodele MO, *et al.* (2020) Evaluation of land use/land cover changes due to gold mining activities from 1987 to 2017 using landsat imagery, East Cameroon. *GeoJournal* 85: 1097–1114.

[6] Gadal S, Gérard P, Gbetkom A, Mfondoum HN, (2021) A new soil degradation method analysis by Sentinel-2 images combining spectral indices and statistics analysis: application to the Cameroonian shores of Lake Chad and its hinterland. In: 7th International Conference on Geographical Information Systems Theory, Applications and Management (GISTAM), Zurich, pp.25-36.

[7] BASIR CM, Hasanah U, Nur I, and Serikawa Y, (2011) Gold Mining Activities and Its Impacts on Land Degradation in Central Sulawesi Indonesia. *Journal of Ecotechnology Research* 16(3-4): 79- 83.

[8] Hill MJ, Braaten R, Veitch SM, Lees BG, Sharma S, (2005) Multi-Criteria Decision Analysis In Spatial Decision Support: the Assess Analytic Hierarchy Process And The Role of quantitative methods and spatially explicit analysis. *Environ. Modell. Softw*. 20: 955–976.

[9] De jong M.S, Freek D, van der M, Jan GPW, Clevers, (2015) Remote Sensing Image Analysis: Including the Spatial Domain, 1–15, Springer

[10] Charou E, Stefouli M, Dimitrakopoulos D, Vasiliou E, Mavrantza O, (2010) Using Remote Sensing to Assess Impact of Mining Activities on Land and Water Resources. *International Journal of Mine Water* 29(1):45-52.

[11] Violeta D, Poenaru C, Alexandru B, et a. (2011) Land degradation monitoring in the Ocnele Mari salt mining area using satellite imagery. University of Agronomical Science and Veterinary Medicine, Bucharest. https: // www.researchgate.net/ publication/235888900_ [accessed Oct 20 2023].

[12] Kiran S, Rohit K, and Kakoli G, (2018). Land Use/Land Cover Dynamics During 2001 And 2021 Using Google Earth Engine and GIS in Ramagundam Coal Mining Area, A Part of Pranhita Godavari Valley, Southern India, Geology Discipline, School of Sciences, Indira Gandhi National Open University, New Delhi, India.

[13] Manga EV, Nchang GN, Suh CE, (2017) Environmental geochemistry of mine tailings soils in the artisanal gold mining district of Bétaré-Oya, Cameroon. Environment and Pollution 6(1):52-61.

[14] Tehna N, Nguene FD, Etame J, Medza EM, Noa Tang S, Suh EC, Bilong P, (2015) Impending Pollution of Bétaré Oya Opencast Mining Environment (Eastern Cameroon). *Journal of Environmental Science and Engineering* B 4: 37-46.

[15] Nodem FR, Sangodoyin AYM, Kegne FN, (2018) Spatial Assessment of Impacts of Artisanal and Small-scale Mining on Land Cover and Environment, Batouri, Eastern Cameroun. *African Journal of Land Policy and Geospatial Sciences* 2 (3): 85-96.

[16] Olsson L, Barbosa H, Bhadwal S, et al. (2019) Land Degradation. In: *Climate Change and Land: an IPCC special report on climate change, desertification, land degradation, sustainable land management, food security, and greenhouse gas fluxes in terrestrial ecosystems*. https://www.ipcc.ch/srccl/: accessed on 20-10-2023 at 2.45 am.

[17] Voundi E, Mbevo PF, Essigue PE (2019) Analyse des mutations socio-environnementales induites par l'exploitation miniere a Betare-Oya, Est-Cameroun. *Vertigo* 19 (1). mis en ligne le 05 mars 2019, consulté le 20 octobre 2023. URL: http:// journals.openedition.org/vertigo/24329.

[18] Temgoua L, Ajonina G, Woyu H, (2018) Land use and land cover change analysis in Ajei Upland Watershed Community Forest, North West Region, Cameroon. *Journal of Geoscience and Environment Protection*, 6: 83-99.

[19] Toteu SF, Penaye J, Poudjom DY, (2004) Geodynamic Evolution of the Pan-African Belt in Central Africa with Special Reference to Cameroon. *Canadian J. Earth Science* 41: 73–85

[20] Mimba ME, Ohba T, Nguemhe SCF, Wirmvem MJ, et al. (2017). Regional Hydrogeochemical Mapping for Environmental Studies in the Mineralized Lom Basin, East Cameroon: A Pre-industrial Mining Survey. *Hydrology* 5 (2): 15-31.

[21] https://earth.esa.int/eogateway/instruments/etm-landsat-7-/products-information/. Accessed on 12-06-2022 at 7.50 pm.

[22] https://www.esa.int/Applications/Observing_the_Earth/Copernicus/Sentinel-2. Accessed on 12-06-2022 at 7.58 pm.

[23] Gascon F, Cadau E, Colin O et al. (2014). Copernicus Sentinel-2 mission: products, algorithms and Cal/Val. In *Earth observing systems XIX* (Vol. 9218, p. 92181E). International Society for Optics and Photonics.

[24] Pei W, Yao S, Knight F. et al. (2017) Mapping and detection of land use change in a coal mining area using object-based image analysis. *Environmental Earth Sciences* 76(3): 125-136.

[25] Denègre J, (2013) *Thematic mapping from satellite imagery: a guidebook*. Elsevier, London.

[26] Sathya P, Baby V, (2019) Classification Process of Satellite Images. *International Journal of Computer Application* 9 (1): 2250-1797.

[27] Rwanga S, Ndambuki J, (2017) Accuracy Assessment of Land Use/Land Cover Classification Using Remote Sensing and GIS. *International Journal of Geosciences* (8): 1-5.

[28] Bogoliubova A, Tymków P, (2014) Accuracy assessment of automatic image processing for land cover classification of St. Petersburg protected area. *Acta Sci. Pol. Geod. Descr. Terr.*, 13 (1-2), 5–22.

[29] Farah A, Algout A, Algouti A, et al. (2021) Mapping of soil degradation in semi-arid environments in the ouarzazate basin in the south of the central High Atlas, Morocco, using Sentinel-2A data. *Remote Sensing Applications: Society and Environment*, 100548.

[30] Jong SMD, Meer FD, Clevers JG (2004). Basics of remote sensing. In *Remote sensing image analysis: Including the spatial domain* (pp. 1-15). Springer, Dordrecht.

[31] Hilson G, Van Bockstael S, Sauerwein T, et al. (2021). Artisanal and small-scale mining, and COVID-19 in sub-Saharan Africa: A preliminary analysis. *World Development* 139: 105315.

[32] Singh RK, Singha M, Singh SK et al. (2018). Land use/land cover change detection analysis using remote sensing and GIS of Dhanbad district, India. *Eurasian Journal of Forest Science* 6(2): 1-12.